Available online at www.sciencedirect.com
SCIENCE DIRECT
Journal of Sound and Vibration 260 (2003) 83–100
JOURNAL OF SOUND AND VIBRATION
www.elsevier.com/locate/jsvi

# An energy residual method for detection of the causes of vibration hypersensitivity

M. Ouisse*, J.L. Guyader

*Laboratoire Vibrations Acoustique, Institut National des Sciences Appliquées de Lyon, Bâtiment St Exupéry, 25 bis avenue J Capelle, 69621 Villeurbanne Cedex, France*

Received 19 November 2001; accepted 11 March 2002

**Abstract**

This work deals with hypersensitive vibration behavior of plates. The aim of the proposed method is to detect structural zones inducing such behavior. It is based on a residual calculation, which takes into account structural uncertainties, and has a low numerical cost since it requires only the resolution of the problem for the nominal structure. Then, this solution is used to calculate energy residuals on different parts of perturbed structures in order to detect which zones will produce an hypersensitive behavior. The basis of the method is first developed on a simple problem, a rod, and then applied to a typical hypersensitive structure, a plates network. Finally, one can show that the proposed tool is able to detect which zones of the plates network are responsible for hypersensitive behavior.
© 2002 Elsevier Science Ltd. All rights reserved.

## 1. Introduction

Because of manufacturing cost, uncertainties in structural parameters are inevitable, bringing dispersions in eigenfrequencies and responses of the structures, which can induce acoustical problems when shifted structural eigenfrequencies are coinciding with cavity ones. In this way, two objects manufactured with the same constraints can have very different acoustical behavior. Fortunately, in most cases, this problem does not exist, and uncertainties in manufacturing processes are expected to entail small variations in eigenvalues, eigenvectors and responses of structures, allowing one to predict the behavior of a set of structures on the basis of results obtained for the nominal one. Hypersensitivity appears when these dispersions become larger,

*Corresponding author. Tel.: +33-472-43-62-15; fax: +33-478-27-87-12.
*E-mail addresses:* ouisse@lva.insa-lyon.fr (M. Ouisse), guyader@lva.insa-lyon.fr (J.L. Guyader).

0022-460X/03/$ - see front matter © 2002 Elsevier Science Ltd. All rights reserved.
PII: S0022-460X(02)00901-X

bringing large differences between the nominal structure and some of other structures belonging to the same manufacturing set. This problem has been raised many times, and many people are interested in reducing dispersion without increasing manufacturing cost. In Ref. [1,2], measurement results are shown on nominally identical structures, and many differences can be observed in the whole frequency domain, although these papers are mainly related to the effects of uncertainties in the high-frequency range. Results presented by Bernhard [2] concern frequency responses for sound pressure due to mechanical excitation for a population of 98 nominally identical vehicles. Large differences can be observed, mostly in medium- and high-frequency ranges. Frequency responses of vibrating 3-beams systems are used to understand these behaviours. Similar results have been presented by Fahy [1], concerning 41 nominally identical structures.

Many existing methods allow one to evaluate dispersion but only when uncertainties are small: statistical dynamics is a classical field of research [3–5]. But if a given parameter is hypersensitive, in other words if a small variation of this parameter brings a large variation of the response, those methods are unable to evaluate the corresponding dispersion. Nevertheless, several efficient ways can estimate the response sensitivity for small variations of parameters. Many stochastic approaches have been developed, some of them need a short calculation time (FORM, SORM), giving good results for small variations in particular cases, while others are more expensive but have a better accuracy and have been developed to be integrated with existing methods, like the finite element method (FEM) [6]. Among new developments, fuzzy methods may be mentioned [7,8]. Like stochastic methods, when the formulation is adapted for large variations of input parameters, a good agreement with real dispersion values can be obtained only if the calculation time is about the same as in a Monte Carlo simulation. This is still the only method capable of estimating correctly the response sensitivity in every case, even if hybrid methods using partial Monte Carlo simulations are considered [9].

An alternative way to these high calculation cost methods for hypersensitivity cases could be to develop a tool that would be able to detect, without high calculation time, which part of the structure causes high sensitivity. This tool could be used to direct a design modification of sensitive parts in order to reduce response dispersions. Following this concept, we have developed a method that is based on only the resolution of the nominal problem, used for estimation of an a posteriori error, which supplies an indicator evaluated for the whole structure, or for different parts of it, and which then allows one to detect causes of hypersensitivity. This paper presents a theoretical background, necessary before an explanation of the method, which is developed in detail on a typical hypersensitive structure.

## 2. Theoretical background

The aim of this part is to present a short description of the tool used here. A simple way to understand the basic ideas of the tool is to consider a simple problem, like a displacement description of a forced longitudinal vibrating structure (Fig. 1). The classical local formulation of the problem can be written in the following terms. The displacement field $U$ must satisfy the

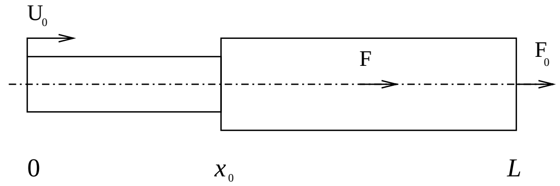


Fig. 1. Rod model.

equation of motion:

$$\frac{d}{dx}\left[ES_1\frac{dU}{dx}\right]+\omega^2\rho S_1 U=0 \quad \text{in } I_1=]0,x_0[, \tag{1}$$

$$\frac{d}{dx}\left[ES_2\frac{dU}{dx}\right]+\omega^2\rho S_2 U=F \quad \text{in } I_2=]x_0,L[. \tag{2}$$

According to the boundary conditions:

$$U_{|x=0}=U_0, \tag{3}$$

$$ES_2\frac{dU}{dx}_{|x=L}=F_0, \tag{4}$$

while continuity of forces and displacements for $x=x_0$ imposes

$$U_{|x=x_0^-}=U_{|x=x_0^+}, \tag{5}$$

$$ES_1\frac{dU}{dx}_{|x=x_0^-}=ES_2\frac{dU}{dx}_{|x=x_0^+}, \tag{6}$$

where $U_0$ is known and the notation $U_{|x=x_0^-}$ indicates the value of $U$ extended by continuity on $x=x_0$ with $x\leqslant x_0$.

Usually, everything in the previous equations is known except the displacement field $U$. The solution $U_{sol}$ of this problem can be calculated with different methods. One way to obtain it, is to find the field that minimizes the residual

$$\begin{aligned}R(U)=&\frac{ES_1}{L}\left(U_{|x=0}-U_0\right)^2+\frac{1}{2}\int_{I_1}\frac{1}{\omega^2\rho S_1}\left(\frac{d}{dx}\left[ES_1\frac{dU}{dx}\right]+\omega^2\rho S_1 U\right)^2 dx\\&+\frac{ES_1}{L}\left(U_{|x=x_0^-}-U_{|x=x_0^+}\right)^2+\frac{L}{ES_1}\left(ES_1\frac{dU}{dx}_{|x=x_0^-}-ES_2\frac{dU}{dx}_{|x=x_0^+}\right)^2\\&+\frac{1}{2}\int_{I_2}\frac{1}{\omega^2\rho S_2}\left(\frac{d}{dx}\left[ES_2\frac{dU}{dx}\right]+\omega^2\rho S_2 U-F\right)^2 dx+\frac{L}{ES_2}\left(ES_2\frac{dU}{dx}_{|x=L}-F_0\right)^2\end{aligned} \tag{7}$$

This residual has interesting properties:

- $R(U)$ is stationary if and only if $U=U_{sol}$, which means that the solution can be found using numerical approaches;
- $R(U)\geqslant 0$ and $R(U_{sol})=0$, which means that the steadiness of the residual is a minimum and that the residual can be used to estimate the quality of a solution. If an approximate solution

field $U_{app}$ has been calculated on the domain $\Omega = [0, L]$, the value of $R(U_{app})$ is a measurement of the difference between $U_{sol}$ and $U_{app}$.

This residual has been derived using natural weighting of the various terms, in order that it could be linked to energy and work expressions, although these weights values are not mathematically necessary to keep the above properties true.

Moreover, a localization of differences between the two fields can be performed using a decomposition of the residual along the rod: $R(U) = R_1(U) + R_2(U) + R_3(U) + R_4(U) + R_5(U)$, where

$$\begin{aligned}
R_1(U) &= \frac{ES_1}{L}\left(U_{|x=0} - U_0\right)^2,\\
R_2(U) &= \frac{1}{2}\int_{I_1} \frac{1}{\omega^2 \rho S_1}\left(\frac{d}{dx}\left[ES_1 \frac{dU}{dx}\right] + \omega^2 \rho S_1 U\right)^2 dx,\\
R_3(U) &= \frac{ES_1}{L}\left(U_{|x=x_0^-} - U_{|x=x_0^+}\right)^2 + \frac{L}{ES_1}\left(ES_1 \frac{dU}{dx}_{|x=x_0^-} - ES_2 \frac{dU}{dx}_{|x=x_0^+}\right)^2,\\
R_4(U) &= \frac{1}{2}\int_{I_2} \frac{1}{\omega^2 \rho S_2}\left(\frac{d}{dx}\left[ES_2 \frac{dU}{dx}\right] + \omega^2 \rho S_2 U - F\right)^2 dx,\\
R_5(U) &= \frac{L}{ES_2}\left(ES_2 \frac{dU}{dx}_{|x=L} + F_0\right)^2.
\end{aligned} \tag{8}$$

If the field $U$ used for the estimation is not $U_{sol}$, at least one of the values of $R_i(U)$ is different from zero, allowing one to know on which part of the structure the field is not correct. Let us note that $R_2$ and $R_4$ can be decomposed in many parts in order to have a better localization of errors.

These expressions are very similar to those which are used for adaptive mesh in vibration analysis. Fundamental works have been presented by Ladevèze and Leguillon [10] and Babuska [11], while Verfurth gives in Ref. [12] an overview of the most popular error estimators. As far as an acoustic field is concerned, Bouillard and Ihlenburg have adapted these methods in Ref. [13].

Another application of error in the constitutive law has been presented by Guyader in Ref. [14], relating to bounding of eigenfrequencies of imperfectly characterized structures. This work shows the validity of the Love–Kirchhoff plate assumption, but as far as bounding is concerned, calculated eigenfrequencies boundaries are unfortunately often very large.

## 3. A method for hypersensitivity cause detection

Many methods are able to determine the sensitivity of a result according to a given parameter, but none of them allows one to detect structural causes of hypersensitivity. This is the aim of this paper. Until now, the only efficient way to detect these causes is to perform a high cost Monte Carlo simulation, solving the problem many times. An alternative way of low numerical cost is proposed here.

First, the problem must be solved with nominal parameters. That is to find the displacement field $U_{sol}$ verifying Eqs. (1)–(6). If the displacement field is a good approximation of the exact solution, then using it in the residual should give a result close to zero.

Then, using residual (8) adapted to the structure, its variable parameters and solution of the nominal problem allows one to estimate the quality of the solution field of the nominal problem in perturbed operators. For each chosen part of the structure on which we perform this post-processing calculation, the estimator indicates the sensitivity according to variable parameters.

This method requires only one resolution of the whole problem, then the nominal solution field is used to perform the calculation of an estimator on perturbed structures.

## 4. A structure with a high sensitivity

To demonstrate the interest of the proposed method, one requires highly sensitive structures. A relatively simple analytic one is a network of plates. Rebillard and Guyader have shown [15] that the sensitivity of two plates (Fig. 2) coupled with an angle $\theta$ was maximum for a nominal value of the connecting angle $\theta$ of $4^\circ$, so the structure presented in Fig. 3 presents three presumed hypersensitive connections, which are numbered 4, 5 and 7. If the connecting angle $\theta$ does not exist, there is no reflected wave, the entire incident one is fully transmitted. As soon as $\theta$ has a non-null value, transmitted power decreases quickly, and coupling effects between in-plane and bending movements imply that the most sensitive angle has a value of $4^\circ$. This value depends on the chosen geometry and structural parameters [16]. The analytical model used is presented in Ref. [15] and consists in a semi-modal decomposition combined to a wave formulation, and takes into account coupling effects between flexural and in-plane motions due to connecting angles.

The steel plates ($E = 2 \times 10^{11}$ Pa, $\eta = 10^{-2}$ $\nu = 0.3$) have a common width of 40 cm and thickness of 2 mm. The structure, which could be a kind of hood of a machine is contained in a box of size $0.4\,\text{m} \times 0.54\,\text{m} \times 1.7\,\text{m}$. The plates are simply supported on the uncoupled sides, and the connecting angles can be classified in two categories: hypersensitive for numbers 4, 5 and 7 (their nominal value is $4^\circ$), while the other ones are not sensitive ($45^\circ$, $86^\circ$ and $90^\circ$ for nominal values).

In order to study the sensitivity of angular parameters, assume that their values are randomly distributed in a $1^\circ$ range around the nominal one. A Monte Carlo simulation allows one to confirm the high sensitivity of the connecting angles. Fig. 4 shows the variability of flexural velocity response of the plate located between angles 7 and 8, when an harmonic excitation is

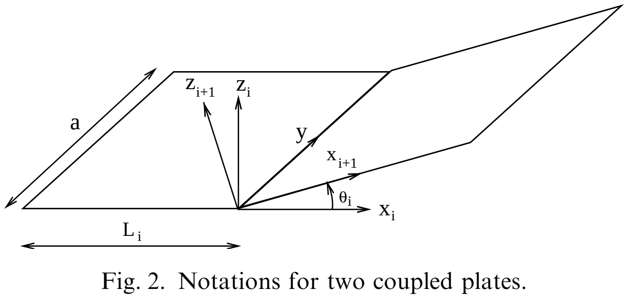


Fig. 2. Notations for two coupled plates.

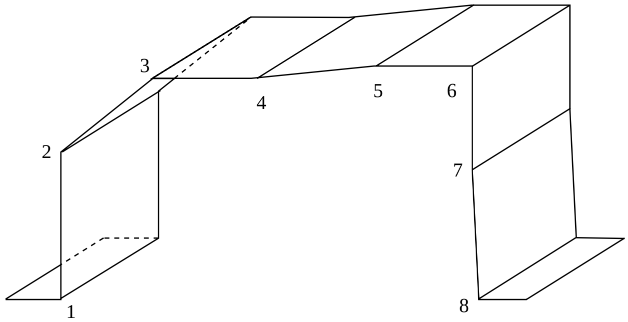


Fig. 3. Steel plates hypersensitive structure.

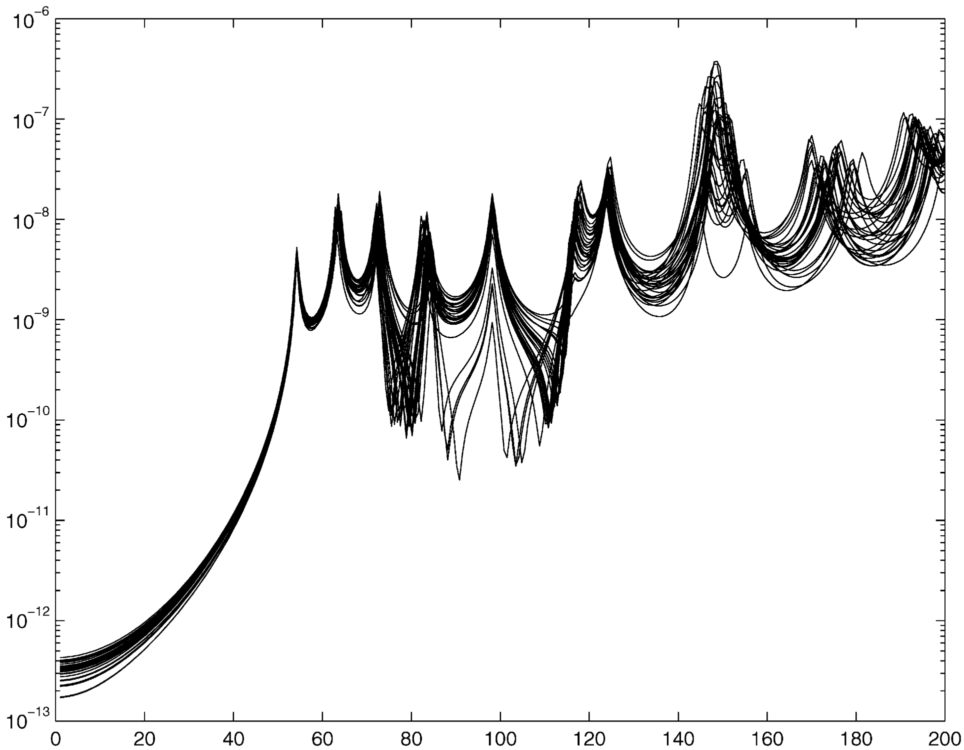


Fig. 4. Displacement responses versus frequency for variation of all connecting angles, 20 cases.

applied to the plate located between angles 1 and 2. Connecting angles 1–8 are chosen in a random way, according to their nominal value with a $1^\circ$ uncertainty (Gaussian distribution, with a $\frac{1^\circ}{6}$ standard deviation).

The sensitivity is important, almost in the band 140–200 Hz. One can determine the influence of each connecting angle in the frequency range 150–200 Hz. Fig. 5 shows the variability of the response when only angle 4 is varying, Fig. 6 for angle 5, Fig. 7 for angle 7. Then, Fig. 8 allows one to conclude that other connecting angles have a very small sensitivity. These remarks are

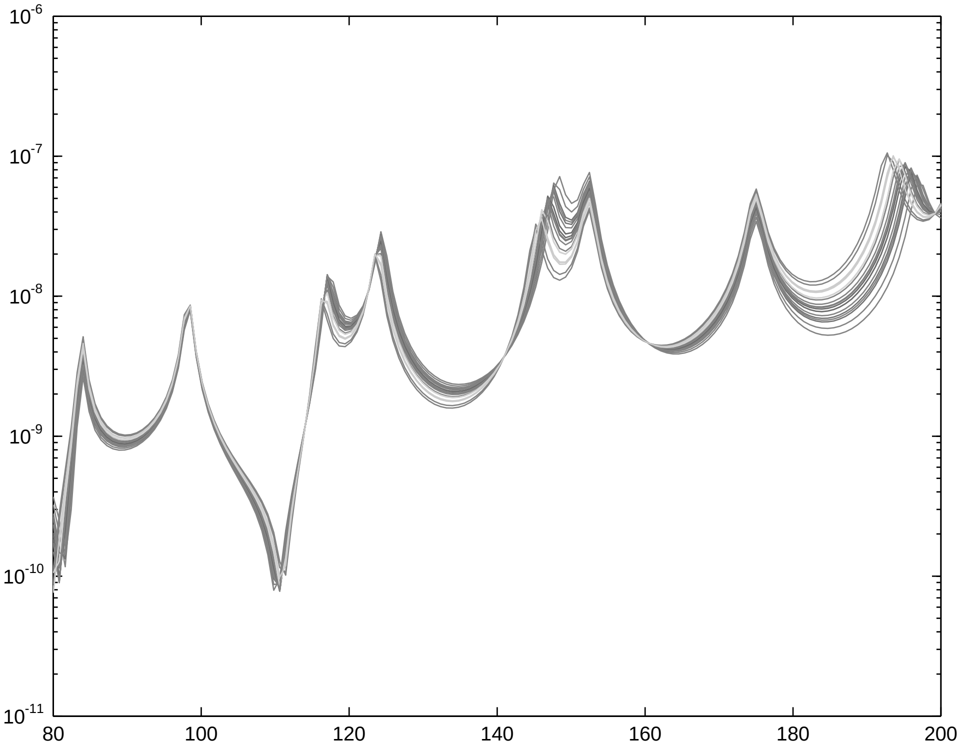


Fig. 5. Sensitivity of connecting angle no. 4. Displacement (m) versus frequency (Hz), 20 cases.

made without using any measure for hypersensitivity, which could be done in many ways. Such a tool could be based among other things on the differences of eigenvalues, or modulus of response at a precise frequency or in a range [15]. One could also take into account one or many statistical moments of variables, but this is not the purpose of this work. What matters here is that the considered structure is highly sensitive to identified parameters, and this can be done easily observing Figs. 5–7.

In conclusion, the developed method should be able to detect, with the residual, the three angles numbered 4, 5 and 7 as hypersensitive ones.

## 5. Application of the method to hypersensitive structures

### *5.1. One simple example: a rod of variable cross-section*

What is to be expected when applying the method is the detection of the connecting angles 4, 5 and 7 as hypersensitive ones. In order to apply the proposed method to the previously presented case, one needs an expression of the residual adapted to plates. However, because the mathematical expression to handle plates is complicated, we first present the simple case of a rod of variable cross-section at point $x_0$, like the one presented in Fig. 1. The equations that have

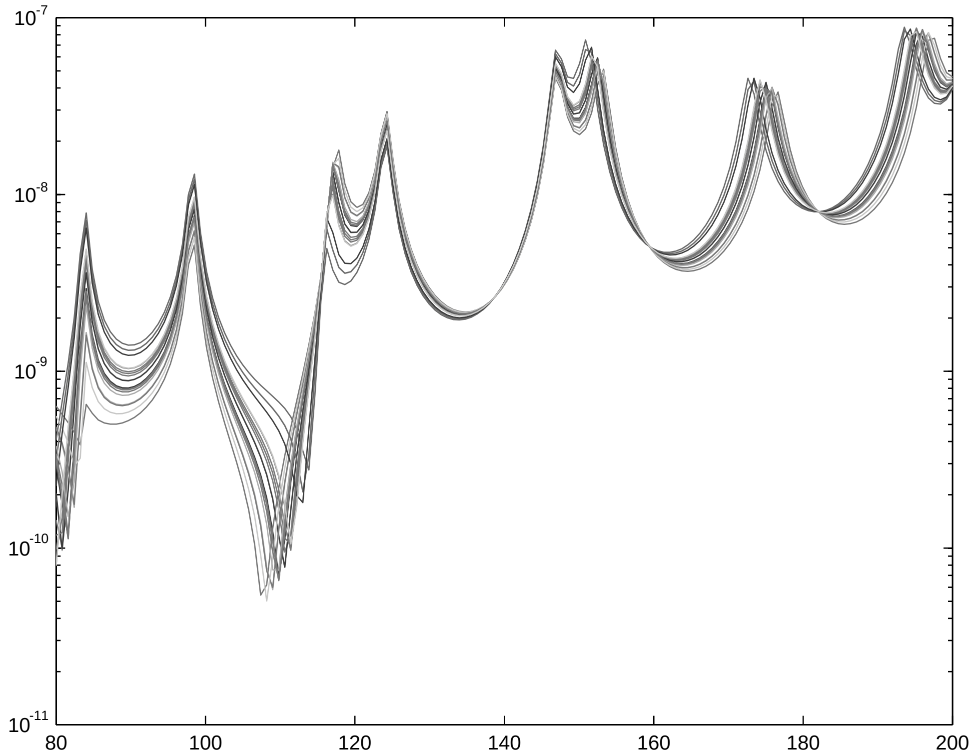


Fig. 6. Sensitivity of connecting angle no. 5. Displacement (m) versus frequency (Hz), 20 cases.

to be satisfied in this case are numbered (1)–(6). The solution $U_{sol}$ of this problem is expected to be known, and of course satisfies Eqs. (1)–(6). Moreover, using this displacement field in residual (7) or (8) produces a null value. Now consider another structure, which is the same as the previous one, except its section size $S_1' \neq S_1$ on part $I_1 = ]0, x_0[$ of the rod. If one considers structural operators of this second rod, using the solution $U_{sol}$ of the first problem produces

$$\frac{\mathrm{d}}{\mathrm{d}x}\left[ES_1'\frac{\mathrm{d}U_{sol}}{\mathrm{d}x}\right] + \omega^2\rho S_1' U_{sol} = 0 \quad \text{in } I_1 = ]0, x_0[, \tag{9}$$

$$\frac{\mathrm{d}}{\mathrm{d}x}\left[ES_2\frac{\mathrm{d}U_{sol}}{\mathrm{d}x}\right] + \omega^2\rho S_2 U_{sol} = F \quad \text{in } I_2 = ]x_0, L[, \tag{10}$$

$$U_{sol\,|x=0} = U_0, \tag{11}$$

$$ES_2\frac{\mathrm{d}U_{sol}}{\mathrm{d}x}_{|x=L} = F_0, \tag{12}$$

$$U_{sol\,|x=x_0^-} = U_{sol\,|x=x_0^+}, \tag{13}$$

$$ES_1'\frac{\mathrm{d}U_{sol}}{\mathrm{d}x}_{|x=x_0^-} \neq ES_2\frac{\mathrm{d}U_{sol}}{\mathrm{d}x}_{|x=x_0^+}. \tag{14}$$

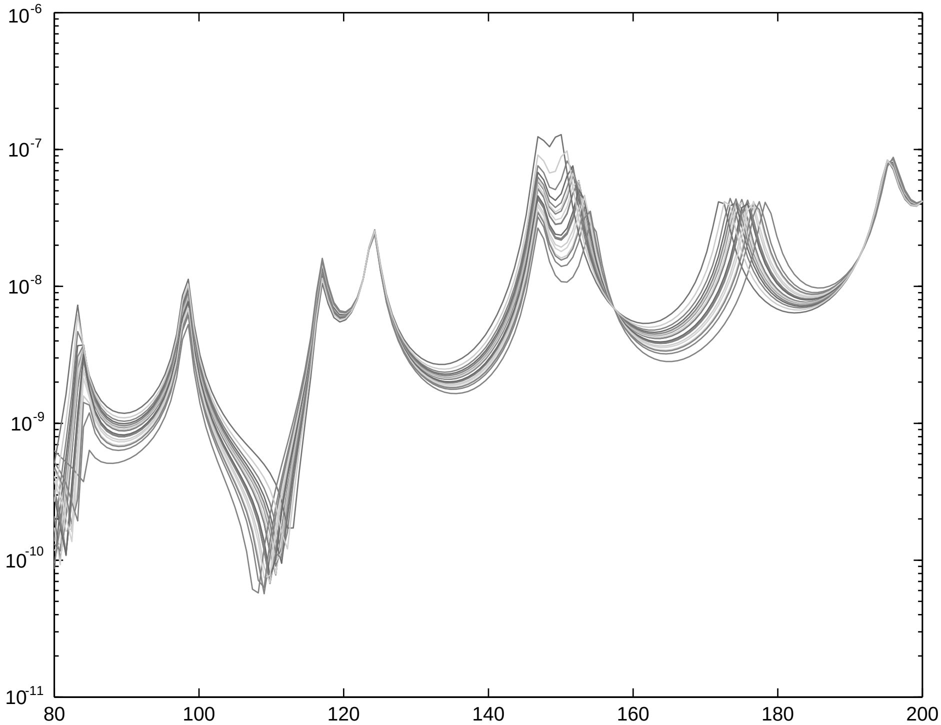


Fig. 7. Sensitivity of connecting angle no. 7. Displacement (m) versus frequency (Hz), 20 cases.

The only equation that $U_{sol}$ does not satisfy is the one relative to continuity of normal force at $x_0$ (Eq. (14)). Using the residual expression (8) adapted to the second structure (using $S_1'$ instead of $S_1$) with solution $U_{sol}$ one obtains

$$
\begin{aligned}
R_1'(U_{sol}) &= \frac{ES_1'}{L}\left(U_{sol\,|x=0} - U_0\right)^2 = 0,\\
R_2'(U_{sol}) &= \frac{1}{2}\int_{I_1}\frac{1}{\omega^2\rho S_1'}\left(\frac{\mathrm{d}}{\mathrm{d}x}\left[ES_1'\frac{\mathrm{d}U_{sol}}{\mathrm{d}x}\right] + \omega^2\rho S_1' U_{sol}\right)^2 \mathrm{d}x = 0,\\
R_3'(U_{sol}) &= \frac{ES_1'}{L}\left(U_{sol\,|x=x_0^-} - U_{sol\,|x=x_0^+}\right)^2 + \frac{L}{ES_1}\left(ES_1'\frac{\mathrm{d}U_{sol}}{\mathrm{d}x}_{|x=x_0^-} - ES_2\frac{\mathrm{d}U_{sol}}{\mathrm{d}x}_{|x=x_0^+}\right)^2 \neq 0,\\
R_4'(U_{sol}) &= \frac{1}{2}\int_{I_2}\frac{1}{\omega^2\rho S_2}\left(\frac{\mathrm{d}}{\mathrm{d}x}\left[ES_2\frac{\mathrm{d}U_{sol}}{\mathrm{d}x}\right] + \omega^2\rho S_2 U_{sol} - F\right)^2 \mathrm{d}x = 0,\\
R_5'(U_{sol}) &= \frac{L}{ES_2}\left(ES_2\frac{\mathrm{d}U_{sol}}{\mathrm{d}x}_{|x=L} + F_0\right)^2 = 0.
\end{aligned}
\qquad (15)
$$

The only part of the residual which is not satisfy zero is the third part $R_3'(U)$. It is related to Eq. (13) (which is satisfied, so the first term of $R_3'$ does vanish) and Eq. (14) (which is not satisfied).

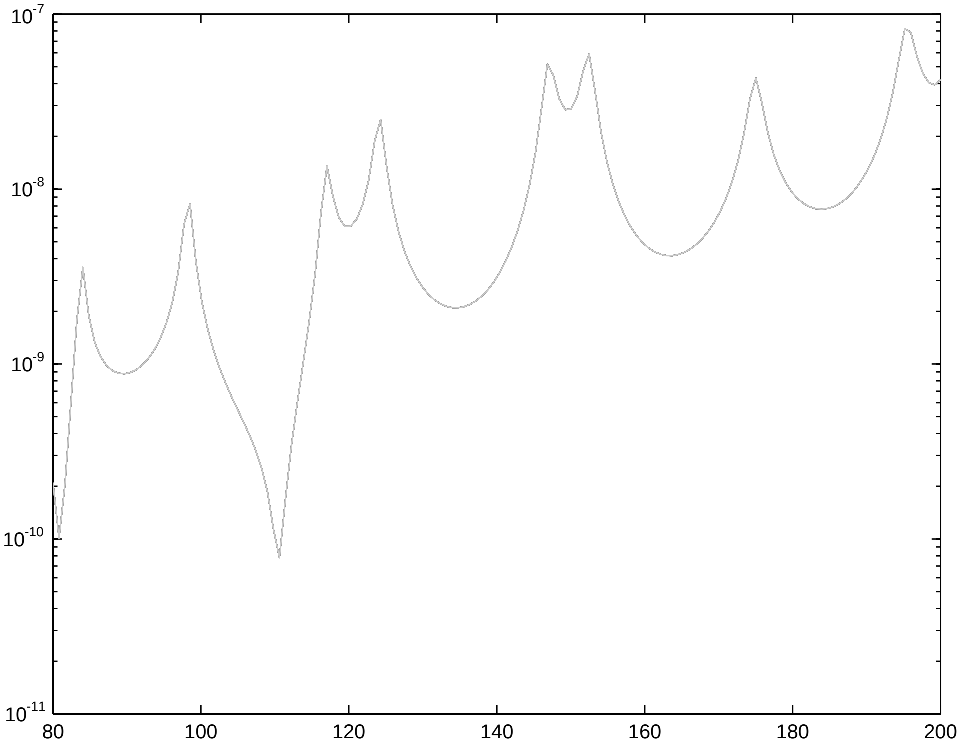


Fig. 8. Sensitivity of other angles. Displacement (m) versus frequency (Hz), 20 cases.

Therefore,

$$R'_3(U_{sol}) = \frac{L}{ES_1}\left(ES'_1\frac{\mathrm{d}U_{sol}}{\mathrm{d}x}_{|x=x_0^-} - ES_2\frac{\mathrm{d}U_{sol}}{\mathrm{d}x}_{|x=x_0^+}\right)^2 \neq 0.$$

Of course this expression has been derived for the 1-D formulation, and needs to be adapted to the plate network problem. But before this derivation, let us remark that the estimator corresponding to $R_3$ that we will use will be a relative one. In order to have a non-dimensional quantity, define

$$e_3(U) = \frac{\frac{ES}{L}\left(U_{|x=x_0^-} - U_{|x=x_0^+}\right)^2 + \frac{L}{ES}\left(ES\frac{\mathrm{d}U}{\mathrm{d}x}_{|x=x_0^-} - ES\frac{\mathrm{d}U}{\mathrm{d}x}_{|x=x_0^+}\right)^2}{\frac{ES}{L}\left(U_{|x=x_0^-} + U_{|x=x_0^+}\right)^2 + \frac{L}{ES}\left(ES\frac{\mathrm{d}U}{\mathrm{d}x}_{|x=x_0^-} + ES\frac{\mathrm{d}U}{\mathrm{d}x}_{|x=x_0^+}\right)^2}. \quad (16)$$

### *5.2. The plate network*

The detailed adapted formulation for the problem is given here, according to the notation defined in Fig. 2. In this part one is interested only in sensitivity due to the connecting angles. All other parameters are supposed to keep their nominal values. This means that the nominal solution satisfies all the equations of the problem with varied angles except continuity conditions at plates junctions. According to that, we will not develop the expression of the whole residual corresponding to Eq. (8), but only the one corresponding to Eq. (16), adapted for the plate network formulation, which is given here. Define: the displacement field on plate $i$: $\vec{U}_i = u_i(x_i, y)\vec{x}_i + v_i(x_i, y)\vec{y} + w_i(x_i, y)\vec{z}_i$, the flexural rotation on plate $i$ along axis $\vec{y}$: $\vec{R}_i.\vec{y} = R_i(x_i, y)$, the generalized forces on plate $i$: $\vec{F}_i = F_{x,i}(x_i, y)\vec{x}_i + F_{y,i}(x_i, y)\vec{y} + F_{z,i}(x_i, y)\vec{z}_i$ and the generalized momentum on plate $i$ along axis $\vec{y}$: $\vec{M}_i.\vec{y} = M_i({}_ix, y)$.

These quantities are linked by the following continuity conditions, which assume rigid connections at plate junctions: $\forall y \in [0, a]$

$$u_{i+1}(0, y) = u_i(l_i, y)\cos\theta_{i+1} + w_i(l_i, y)\sin\theta_{i+1} = u_i^*(l_i, y), \tag{17}$$

$$v_{i+1}(0, y) = v_i(l_i, y), \tag{18}$$

$$w_{i+1}(0, y) = w_i(l_i, y)\cos\theta_{i+1} - u_i(l_i, y)\sin\theta_{i+1} = w_i^*(l_i, y), \tag{19}$$

$$F_{x,i+1}(0, y) = F_{x,i}(l_i, y)\cos\theta_{i+1} + F_{z,i}(l_i, y)\sin\theta_{i+1} = F_{x,i}^*(l_i, y), \tag{20}$$

$$F_{y,i+1}(0, y) = F_{y,i}(l_i, y), \tag{21}$$

$$F_{z,i+1}(0, y) = F_{z,i}(l_i, y)\cos\theta_{i+1} - F_{x,i}(l_i, y)\sin\theta_{i+1} = F_{z,i}^*(l_i, y), \tag{22}$$

$$R_{i+1}(0, y) = R_i(l_i, y), \tag{23}$$

$$M_{i+1}(0, y) = M_i(l_i, y). \tag{24}$$

Note that the star symbol (e.g., in $u_i^*(l_i, y)$) is used here in order to simplify notations, and that all equations must be satisfied $\forall y \in [0, a]$. Then one can define the following estimator, based on expression (16):

$$\begin{aligned} e = {} & \frac{\int_{\partial\Omega} \frac{Eh}{a(1-\nu^2)}(u_{i+1} - u_i^*)^2\,\mathrm{d}\Omega + \int_{\partial\Omega} \frac{Eh}{2a(1+\nu)}(v_{i+1} - v_i^*)^2\,\mathrm{d}\Omega + \int_{\partial\Omega} \frac{D}{a^3}(w_{i+1} - w_i^*)^2\,\mathrm{d}\Omega}{\int_{\partial\Omega} \frac{Eh}{a(1-\nu^2)}(u_{i+1} + u_i^*)^2\,\mathrm{d}\Omega + \int_{\partial\Omega} \frac{Eh}{2a(1+\nu)}(v_{i+1} + v_i^*)^2\,\mathrm{d}\Omega + \int_{\partial\Omega} \frac{D}{a^3}(w_{i+1} + w_i^*)^2\,\mathrm{d}\Omega} \\ & + \frac{\cdots + \int_{\partial\Omega} \frac{a(1-\nu^2)}{Eh}(F_{x,i+1} - F_{x,i}^*)^2\,\mathrm{d}\Omega + \int_{\partial\Omega} \frac{2a(1+\nu)}{Eh}(F_{y,i+1} - F_{y,i}^*)^2\,\mathrm{d}\Omega}{\cdots + \int_{\partial\Omega} \frac{a(1-\nu^2)}{Eh}(F_{x,i+1} + F_{x,i}^*)^2\,\mathrm{d}\Omega + \int_{\partial\Omega} \frac{2a(1+\nu)}{Eh}(F_{y,i+1} + F_{y,i}^*)^2\,\mathrm{d}\Omega} \\ & + \frac{\cdots + \int_{\partial\Omega} \frac{a^3}{D}(F_{z,i+1} - F_{z,i}^*)^2\,\mathrm{d}\Omega + \int_{\partial\Omega} \frac{D}{a}(R_{i+1} - R_i^*)^2\,\mathrm{d}\Omega + \int_{\partial\Omega} \frac{a}{D}(M_{i+1} - M_i^*)^2\,\mathrm{d}\Omega}{+ \int_{\partial\Omega} \frac{a^3}{D}(F_{z,i+1} + F_{z,i}^*)^2\,\mathrm{d}\Omega + \int_{\partial\Omega} \frac{D}{a}(R_{i+1} + R_i^*)^2\,\mathrm{d}\Omega + \int_{\partial\Omega} \frac{a}{D}(M_{i+1} + M_i^*)^2\,\mathrm{d}\Omega}, \end{aligned} \tag{25}$$

where integration domains $\partial\Omega$ are coupling lines and $a$ is the common width of the plates. With such an expression, the method can now be applied to the plate network.

The first step is the resolution of the nominal system, using semi-modal decomposition. For a given frequency, the calculation provides the solution field on the structure. See Ref. [15] for details.

To perform the second step, variable parameters must be defined. In the present case, these are connecting angles. So each angle is supposed to have a Gaussian distribution, on a $1^\circ$ width range

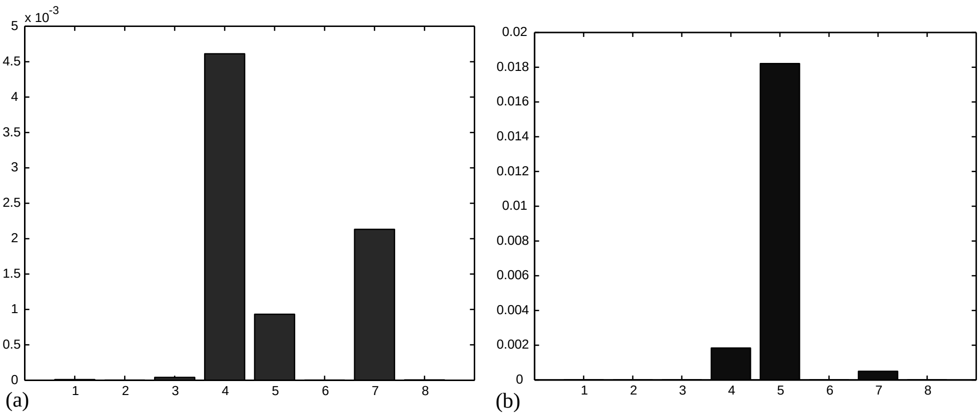


Fig. 9. Residual value vesus connecting angle number, mean of 40 calculations: (a) $f = 175$ Hz and (b) $f = 195$ Hz.

($\frac{1^\circ}{6}$ standard deviation). Locations chosen for the evaluation of the estimator are the coupling lines. For each of these the calculation of expression (25) is carried out, using the displacement field solution of the nominal problem. These calculations are performed using angles randomly chosen in the range, and finally the mean of 40 evaluations for each coupling line is presented, for both frequencies 175 and 195 Hz.

Fig. 9 clearly shows that the estimator is able to detect connecting angles which bring hypersensitive behavior. Using the nominal solution field in a perturbed estimator produces a near zero result for all angles except as those with a nominal value of $4^\circ$ which have a large residual.

## 6. Fast hypersensitivity detection

The first aim of the method is a fast detection of hypersensitive zones, so the number of cases used for evaluation of the mean of estimators should be small, since calculation time grows up with the number of cases. The method is then applied with only three evaluations of the estimators. Fig. 10 clearly shows that two consecutive calculations do not give the same results, which is obvious considering the high sensitivity of parameters. Nevertheless, each of the three hypersensitive zones can be detected, allowing one to obtain a very fast detection of these areas.

## 7. Hypersensitivity causes versus frequency

The presented method allows one to determine sensitivity causes for several frequencies. The calculation performed in a frequency range are presented in Fig. 11, which shows the influence of connecting angles versus frequency, in the 80–200 Hz band. The agreement with Figs. 4–6 is good, since each time the estimator indicates a low value, the sensitivity of the parameter is weak. This can be observed for angle 4 at 115 Hz or for angle 5 at 142 Hz. Large values of residual indicates that the connecting angle is highly sensitive, but the value itself has not been related to any

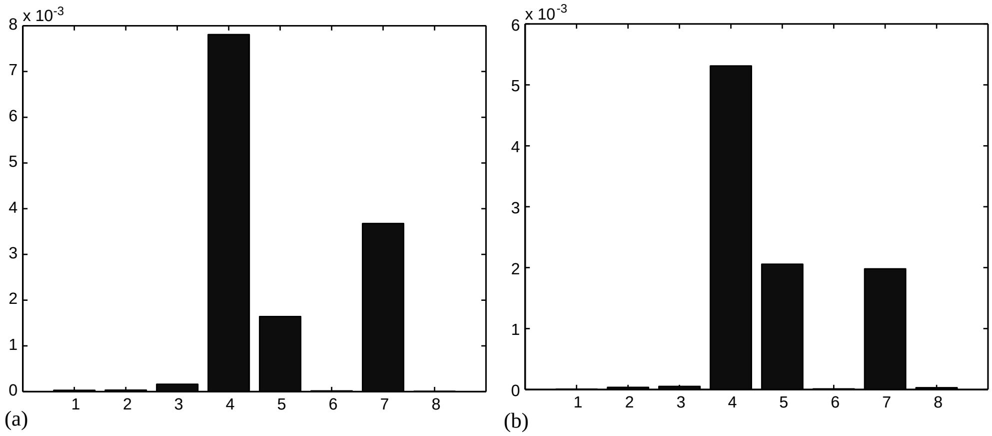


Fig. 10. Residual value versus connecting angle number, mean of 3 cases, $f = 195$ Hz: (a) 1st calculation, (b) 2nd calculation.

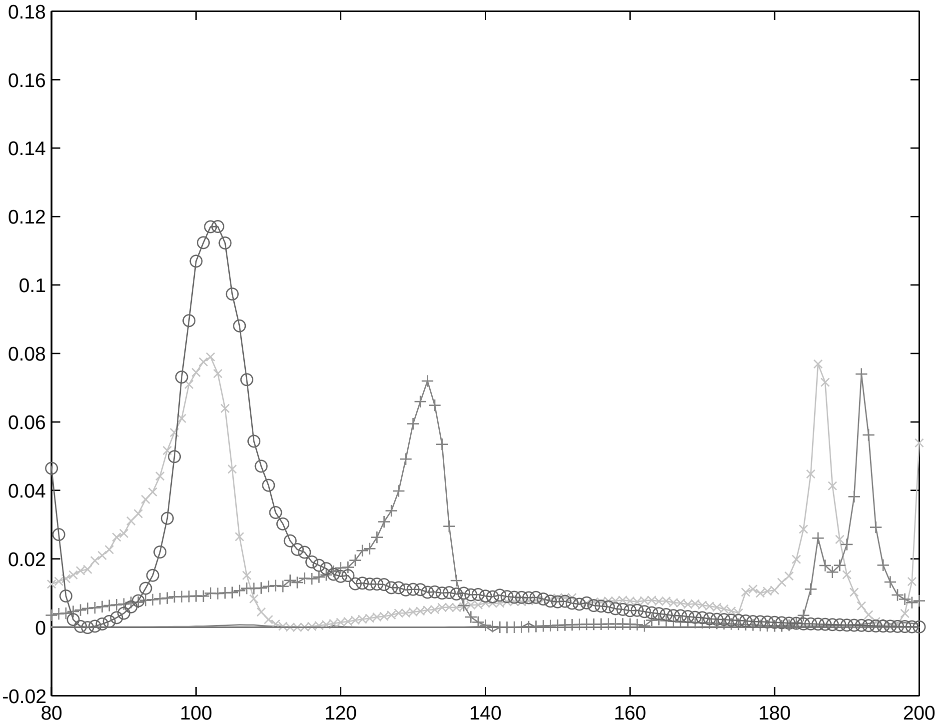


Fig. 11. Residual value versus frequency. Monte Carlo simulation 2000 cases: -x-, angle 4; - + -, angle 5; -o-, angle 7; —, other angles.

sensitivity value of the response. As far as connecting angle 7 is concerned, the residual indicates that its sensitivity goes down between 150 and 200 Hz, and this is in agreement with Fig. 6. On the other hand, for particular frequencies like 125 Hz (for angle 7), the Monte Carlo analysis

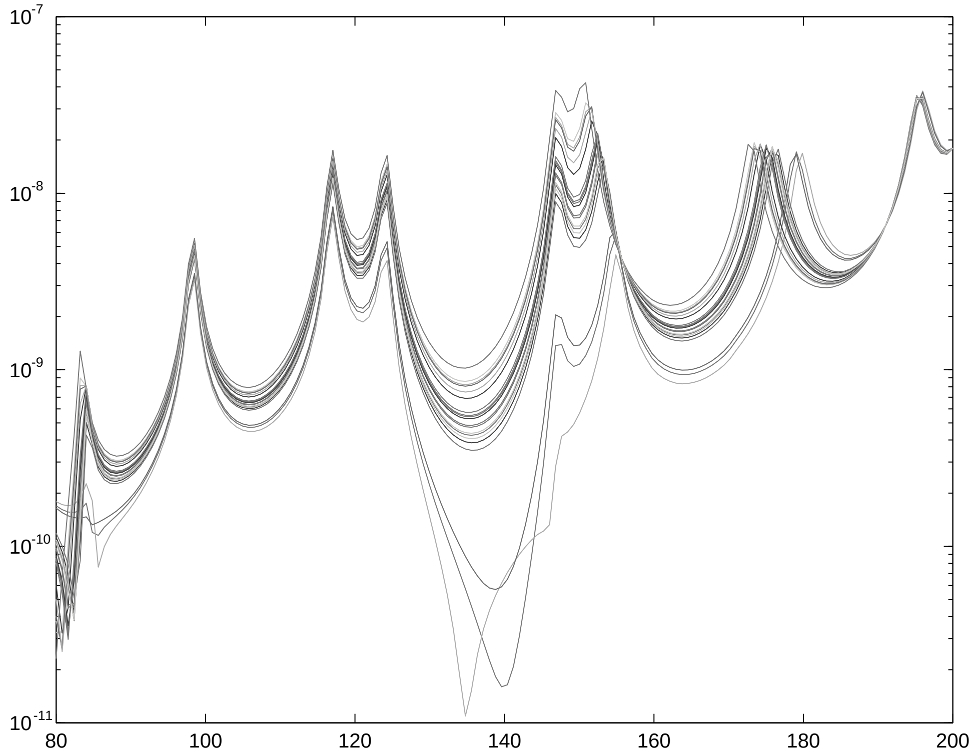


Fig. 12. Sensitivity of connecting angle no. 7. Displacement (m) versus frequency (Hz), 20 cases.

seems to show that the sensitivity is weak, whereas the estimator is not able to detect it. The reason for this difference is that the proposed estimators are global ones, and take into account the solution field on whole structure, even if the post-processing calculation are performed only on a part of it, whereas sensitivity Figs. 4–6 are obtained with a calculation at a particular point of the structure. This means that if one performs another Monte Carlo calculation with the same excitation as the one used for Fig. 6, but measuring displacement response on another point on the same plate, the parameter will be more sensitive, as shown in Fig. 12. This phenomenon can be easily understood if the point used for the evaluation of estimator is located on a node.

## 8. First order analysis of estimators

As far as the present particular structure is concerned, it is possible to obtain an analytical expression of the mean of estimators, using a first order decomposition relating to varying angle. Suppose that the connecting angle $\theta = \bar{\theta} + \theta'$ has a nominal value $\bar{\theta}$ and that its variation is $|\bar{\theta} - \theta'| \ll 1$. The first order estimation of Eq. (25) is developed here. The fields which are not signed with a star are supposed to satisfy Eqs. (17)–(24), according to angle $\bar{\theta}$ while those with a star do not exactly verify them, because of $\theta$.

The first step is to evaluate the first term of Eq. (25) using Eq. (17):

$$(u_{i+1}(0,y) - u_i^*(L_i,y))^2 = (u_{i+1} - u_i\cos\theta - w_i\sin\theta)^2$$

Using the first order decomposition of sinusoidal functions $\cos\theta \simeq \cos\bar\theta - \theta'\sin\bar\theta$ and $\sin\theta \simeq \sin\bar\theta + \theta'\cos\bar\theta$ brings

$$(u_{i+1} - u_i^*)^2 = \theta'^2(u_i\sin\bar\theta - w_i\cos\bar\theta)^2$$

As far as the fields relating to the $y$-axis are concerned, the assumption is that the nominal calculation is correct, so that Eqs. (18), (21), (23), and (24) are satisfied:

$$v_{i+1} - v_i^* = 0, \qquad F_{y,i+1} - F_{y,i}^* = 0,$$

$$R_{i+1} - R_i^* = 0, \qquad M_{i+1} - M_i^* = 0.$$

A similar calculation can be performed in order to estimate the other terms of the numerator in Eq. (25) and lastly, assuming that zeroth order terms are larger than first order one, the evaluation of the estimator is

$$e = \frac{\int_{\partial\Omega}\theta'^2[\frac{Eh}{a(1-\nu^2)}(u_i\sin\bar\theta - w_i\cos\bar\theta)^2 + \frac{D}{a^3}(u_i\cos\bar\theta + w_i\sin\bar\theta)^2}{4\int_{\partial\Omega}[\frac{Eh}{a(1-\nu^2)}u_{i+1}^2 + \frac{Eh}{2a(1+\nu)}v_{i+1}^2 + \frac{D}{a^3}w_{i+1}^2 + \frac{D}{a}R_{i+1}^2}$$

$$\frac{+\cdots + \frac{a(1-\nu^2)}{Eh}(F_{x,i}\sin\bar\theta - F_{z,i}\cos\bar\theta)^2 + \frac{a^3}{D}(F_{x,i}\cos\bar\theta + F_{z,i}\sin\bar\theta)^2]\,\mathrm{d}\Omega}{+\cdots + \frac{a(1-\nu^2)}{Eh}F_{x,i+1}^2 + \frac{2a(1+\nu)}{Eh}F_{y,i+1}^2 + \frac{a^3}{D}F_{z,i+1}^2 + \frac{a}{D}M_{i+1}^2]\,\mathrm{d}\Omega}.$$

Considering only the first order estimation, this estimator is proportional to $\theta'^2$ and a statistical calculation can be performed to determine its mean. Denoting $\sigma_{\theta'}$ the standard deviation of $\theta'$ and assuming a Gaussian centered distribution:

$$f_{\theta'}(\mu) = \frac{1}{\sigma_{\theta'}\sqrt{2\pi}}\exp\left(-\frac{\mu^2}{2\sigma_{\theta'}^2}\right),$$

one can calculate the distribution of $\theta'^2$, which is zero on $]-\infty, 0[$, and on $]0, +\infty[$ :

$$f_{\theta'^2}(\mu) = \frac{1}{\sigma_{\theta'}\sqrt{2\pi\mu}}\exp\left(-\frac{\mu}{2\sigma_{\theta'}^2}\right).$$

This can be found using the cumulative distribution function $F_{\theta'^2}(k) = P(\theta'^2 \leqslant k) = P(-\sqrt{k} \leqslant \theta' \leqslant \sqrt{k})$

$$F_{\theta'^2}(k) = \int_{-\sqrt{k}}^{+\sqrt{k}} f_{\theta'}(\mu)\,\mathrm{d}\mu = \int_0^{\sqrt{k}} \frac{2}{\sigma_{\theta'}\sqrt{2\pi}}\exp\left(-\frac{\mu^2}{2\sigma_{\theta'}^2}\right)\mathrm{d}\mu$$

using the substitution $t = \mu^2$ brings:

$$F_{\theta'^2}(k) = \int_0^k \frac{1}{\sigma_{\theta'}\sqrt{2\pi t}}\exp\left(-\frac{t}{2\sigma_{\theta'}^2}\right)\mathrm{d}t.$$

Then one can evaluate the mean of $\theta'^2$:

$$E(\theta'^2) = \int_0^\infty \mu f_{\theta'^2}(\mu)\,\mathrm{d}\mu = \sigma^2_{\theta'} \frac{2}{\sqrt{\pi}} \int_0^\infty \exp(-t^2)\,\mathrm{d}t = \sigma^2_{\theta'}$$

Finally, this brings one to estimate the first order mean of the residual:

$$e_{\text{first order}} = \sigma^2_{\theta'} \frac{\int_{\partial\Omega}[\frac{Eh}{a(1-\nu^2)}(u_i \sin\bar{\theta} - w_i \cos\bar{\theta})^2 + \frac{D}{a^3}(u_i \cos\bar{\theta} + w_i \sin\bar{\theta})^2}{4\int_{\partial\Omega}[\frac{Eh}{a(1-\nu^2)}u^2_{i+1} + \frac{Eh}{2a(1+\nu)}v^2_{i+1} + \frac{D}{a^3}w^2_{i+1} + \frac{D}{a}R^2_{i+1}}$$
$$\frac{+\cdots + \frac{a(1-\nu^2)}{Eh}(F_{x,i}\sin\bar{\theta} - F_{z,i}\cos\bar{\theta})^2 + \frac{a^3}{D}(F_{x,i}\cos\bar{\theta} + F_{z,i}\sin\bar{\theta})^2]\,\mathrm{d}\Omega}{+\cdots + \frac{a(1-\nu^2)}{Eh}F^2_{x,i+1} + \frac{2a(1+\nu)}{Eh}F^2_{y,i+1} + \frac{a^3}{D}F^2_{z,i+1} + \frac{a}{D}M^2_{i+1}]\,\mathrm{d}\Omega}. \quad (26)$$

This expression allows one to have a very fast means of obtaining the estimator frequency evolution, since only one post-processing calculation has to be performed. Fig. 13 shows the frequency evolution of estimator (2), and has to be compared with Fig. 11. The first order estimation is close to the Monte Carlo simulation. The small differences are due to higher order terms, but the first order estimation is close to the expected result.

Finally, for this particular case, the first order analysis is a very fast way to obtain pertinent informations about frequency evolution of the estimator. One should be precise that this first

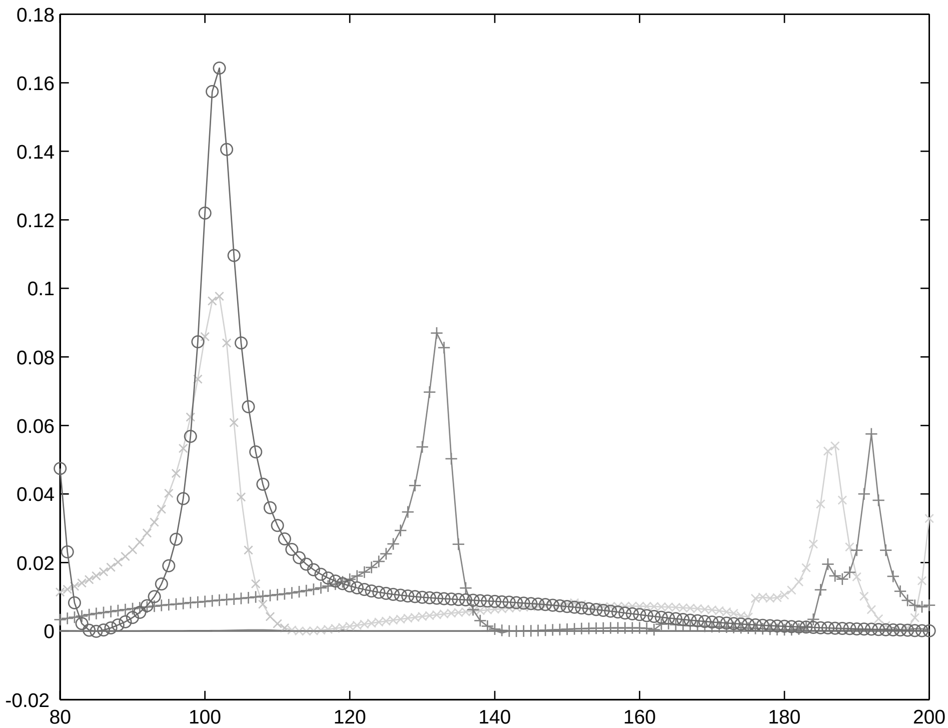


Fig. 13. Evolution of first order linearization of residual value versus frequency.

order analysis is not necessary to find structural zones which are responsible for hypersensitive behavior, as shown in Section 6. Nevertheless, it allows one to obtain more precise results. In the present case, there is only one structural parameter which is supposed to vary, and the first order analysis expression is quite easy to obtain. For a different structure, with many varying parameters, it could be that it is impossibile to obtain an analytical expression of the estimator like Eq (26). In this case the estimator should be evaluated numerically, with the calculation cost growing with the number of parameters. However, if one is interested only in first order estimation, the computational time will be much less than a Monte Carlo approach.

## 9. Conclusions

A new tool has been presented for the detection of causes of vibration hypersensitivity. It is based on the concept of post-processing error estimation, since only the nominal problem is solved, then the solution is used in a residual functional to localize hypersensitive zones. After a short theoretical background, a specific formulation has been developed and tested on a hypersensitive structure. The proposed method is able to detect hypersensitive zones of the structure, for the studied case three particular connecting angles have been successfully localized. A quick analysis can be performed in order to have a fast estimation of hypersensitive zones, even if results cannot be very precise. Another point is that the tool is able to supply a frequency evolution of hypersensitive zones, and for a particular structure a first order analysis has been performed and brings satisfactory results. The next step in the evolution of the method will be an FEM implementation.

## References

[1] F. Fahy, Statistical energy analysis: a wolf in sheep's clothing? Proceedings of Inter-Noise 93, Vol. 1, Leuven, Belgium, 1993, pp. 13–26.
[2] R. Bernhard, The limits of predictabiliy due to manufacturing and environmentally induced uncertainty, Proceedings of Inter-Noise 96, Liverpool, England, 1996, pp. 2867–2872.
[3] P. Caravani, W. Thomas, Frequency response of a dynamic system with statistical damping, American Institute of Aeronautics and Astronautics Journal 11 (2) (1973) 170–173.
[4] P. Chen, W. Soroka, Multidegree dynamic response of a system with statistical properties, Journal of Sound and Vibration 37 (4) (1974) 547–556.
[5] R. Ibrahim, Structural dynamics with parameters uncertainties, Applied Mechanics Revue 40 (3) (1987) 309–328.
[6] R. Ghanem, P. Spanos, Stochastic Finite Elements: A Spectral Approach, New York, Springer, Berlin, 1991.
[7] S. Rao, J. Sawyer, Fuzzy finite elements approach for the analysis of imprecise defined systems, American Institute of Aeronautics and Astronautics Journal 33 (12) (1995) 2364–2370.
[8] D. Moens, D. Vandepitte, A method for the calculation of fuzzy frequency response functions of uncertain structures based on modal superposition, Proceedings of Euromech 405: Numerical Modelling of Uncertainties, Presses Universitaires de Valenciennes, Valencienne, 1999, pp. 93–101.
[9] E. Blain, D. Aubry, P. Chove, P. Lardeur, Influence of parameters dispersion on the vibrating behaviour of spot welded plates, Proceedings of Euromech 405: Numerical Modelling of Uncertainties, Presses Universitaires de Valenciennes, Valencienne, 1999, pp. 1–6.
[10] P. Ladevèze, D. Leguillon, Error estimate procedure in the finite element method and applications, SIAM Journal on Numerical Analysis 20 (1983) 485–509.

[11] I. Babuska, A posteriori error estimates for the finite element method, International Journal for Numerical Methods in Engineering 12 (1978) 1597–1615.
[12] R. Verfurth, A review of a posteriori error estimation techniques for elasticity problems, Computer Methods in Applied Mechanics and Engineering 176 (1999) 419–440.
[13] P. Bouillard, F. Ihlenburg, Error estimation and adaptivity for the finite element method in acoustics: 2D and 3D applications, Computer Methods in Applied Mechanics and Engineering 176 (1999) 147–163.
[14] J.L. Guyader, Free vibrations of imperfectly characterized elastic continuous media. Application to the validity of Love–Kirchhoff plate assumption, Journal of Theoretical and Applied Mechanics 6 (2) (1987) 231–252.
[15] E. Rebillard, J.L. Guyader, Vibrational behaviour of a population of coupled plates: hypersensitivity to the connexion angle, Journal of Sound and Vibration 188 (3) (1995) 435–454.
[16] M. Ouisse, J.L. Guyader, Vibration sensitive behavior to connecting angle. Case of coupled beams and plates, Journal of Sound and Vibration, to appear.